Pinning stationary planar fronts in diffusion-convection-reaction systems

Moshe Sheintuch, Yelena Smagina, and Olga Nekhamkina
Department of Chemical Engineering, Technion, Haifa 32000, Israel
(Received 21 August 2002; published 20 December 2002)

This paper considers various strategies for controlling a stationary planar front solution, in a rectangular domain with a diffusion-reaction distributed system, by pinning the solution to one or few points and using actuators with the simplest possible spatial dependence. We review previous results obtained for one-dimensional diffusion-reaction (with or without convection) systems, for which we applied two approaches: an approximate model reduction to a form that follows the front position while approximating the front velocity, and linear stability analysis. We apply the same two approaches for the planar fronts. The approximate model reduction allows us to analyze qualitatively various control strategies and to predict the critical width below which the control mode of the one-dimensional system is sufficient. These results are corroborated by linear analysis of a truncated model with the spectral methods representation, using concepts of finite and infinite zeros of linear multidimensional systems.

DOI: 10.1103/PhysRevE.66.066213 PACS number(s): 05.45.Gg, 02.30.Yy, 07.05.Dz

I. INTRODUCTION

This paper is part of a research effort aimed at developing a control theory and its applications for one- and two-dimensional planar distributed systems for which a certain patterned state is advantageous or inevitable. Propagating fronts [1–5] and patterned states, composed of slow-moving fronts, separated by domains of moderate changes, may emerge in several technologies including catalytic reactors [6–8], distillation processes [9], flame propagation, and crystal growth [10]. Patterned states are also of importance in many physiological systems [11]. The research addressed the following questions. (a) What is the class of patterned states that can be maintained by control in a reaction-convection-diffusion system. We can classify most states either as steady in time or homogeneous in space or both, or as steady but inhomogeneous (e.g., front or multifront) states or as moving patterned states (e.g., pulses, spiral waves). Here we are interested mainly in stationary fronts; these are typically characterized by a small number of positive eigenvalues in the uncontrolled one-dimensional (1D) system and can be easily controlled, while lateral instability of planar fronts may add more positive eigenvalues in a sufficiently wide system. (b) What control variables are able to provide the desired patterns? The answer to this question is specific to the physicochemical characteristics of the system in question. (c) What strategy of control should be applied? The answer to the latter is also technology-specific but the control should be made as simple as possible in terms of the number of sensors or actuators and the space dependence of the actuator. We typically assume that sensors measure the local state while actuators may affect a narrow spot, a narrow strip in the plane, or the whole plane; in the limit we can refer to these actuators as point, line, and planar actuators.

We have addressed increasingly complex reactors for which possible patterns, in the absence of control, are known. We have analyzed the control of one-dimensional reaction-diffusion [12,14,15] and reaction-diffusion-convection [13,16] systems, using an approximate model-reduction approach [13,14,16] or a formal numerical approach [15] as described below. The latter corroborates the former, which yields rigorous results in a certain domain, but the latter approach is essential for other ranges of parameters (see below).

The problem of finite-dimensional control of systems that are described by 1D reaction-diffusion equations has been attracting considerable attention. The dissipative nature of the underlying PDE's suggests that the long-term dynamics is low-dimensional. Several approaches for model reduction have been suggested (see references in [17]); recent approaches were based on the central manifold theorem. This formal approach, as well as the linear analysis, does not support any qualitative understanding of the wave behavior of such a system to suggest efficient modes of control. The approach taken in our previous work [16] is different from that applied in most studies: we employed an approximate model reduction to a form that follows the front position while approximating the front velocity.

The purpose of this work is to summarize previous results and extend the results to two-dimensional systems using a simple control procedure that pins the solution to a desired set of points. We already implied that the system state is measured at few certain spots. The planar actuator can act globally and be uniform in space or be space-dependent; the former is easy to implement (e.g., by cooling the whole system) but may be insufficient in a long or wide system. The latter approach, which is more technically challenging, is very efficient when the actuator spatial structure is an imprint of the desired state. In certain uncommon systems (e.g., the potential in electrochemical systems), the actuator can act (almost) locally and in that case we can pin the solution to a desired state. This possibility is not addressed here. The intermediate case of a line actuator in a planar domain may be difficult to implement but may serve as an asymptotic analysis.

In [14] we have analyzed the stability of one-dimensional patterns in one- or two-variable reaction-diffusion systems, by analyzing the interaction between adjacent fronts and between fronts and the boundaries in bounded systems. We have used model reduction to a presentation that follows the

 ©2002 The American Physical Society

front positions, while using approximate expressions for front velocities in order to study various control modes in such systems. These results were corroborated by few numerical experiments. This approach is implemented here as well.

A stationary single front or a pattern with n fronts was shown to be typically unstable due to the interaction between fronts [14]. The two simplest control modes, global control (with a system-averaged sensor) and point-sensor control (pinning), use a single sensor and a single space-independent actuator and will arrest a front in a single-variable problem since both control modes respond, in fact, to front position. In a two-variable system incorporating a localized inhibitor, in the domain of bistable kinetics, global control was shown to stabilize a single front only in short systems while point-sensor control can arrest such a front in any system size. Neither of these control modes can stabilize an n-front pattern (in either one- or two-variable systems), and that task calls for a distributed actuator. A single space-dependent actuator, that is, spatially qualitatively similar to the patterned set point, and which responds to the sum of deviations in sensor readings, was shown to stabilize a pattern that approximately overlaps with the desired state.

The stabilization of a front pattern in a homogeneous tubular reactor model by manipulating various reactor parameters, including fluid flow and feed conditions, was studied in [13]. Point-sensor control by manipulating the heat-loss coefficient or the coolant temperature was shown to be effective when the temperature sensor is located close to the front position. Global control based on a space-averaged sensor failed, as did several other strategies.

The structure of this work is the following. Results of control in a one-dimensional system are reviewed below using a polynomial kinetic model that was previously employed in [14]. These results are extended in Sec. III to planar systems using an approximate model reduction approach as well as a linear analysis, and they are verified by typical simulations. In a future publication, we will apply this know-how to the stabilization of a planar front in a cylindrical annular reactor in which a first-order Arrhenius reaction occurs. This will extend our previous one-dimensional study of this problem [13].

II. ONE-DIMENSIONAL MODELS AND THEIR CONTROL

In [16], we have analyzed three one-dimensional reactors—the adiabatic reactor, the cross-flow reactor, and the catalytic wire or ribbon—and showed that these three situations can be further simplified to a formal model of the form

$$y_t - y_{zz} + V y_z = P(y,\theta,\lambda),$$

$$V(y|_o - y_{\mathrm{in}}) = y_z|_o, \quad y_z|_L = 0, \tag{1a}$$

where y is the state variable (typically the temperature), θ is a nondiffusing (localized) variable (catalytic activity) that is described below, and λ is the control variable. The three situations described above differ in the absence or presence of convection ($V=0$ in the catalytic wire while $V\neq 0$ in the two reactor models) and in the bistability features of $P(y)=0$. The boundary conditions are the well-accepted Danckwerts conditions, which reduce to no-flux conditions in the catalytic wire.

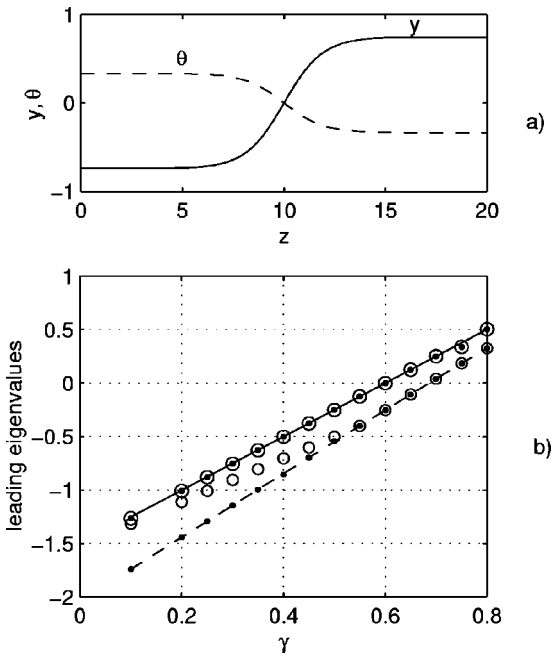

FIG. 1. (a) A typical 1D solution of the reaction-diffusion system [Eq. (1)]; the instability stems from the anticlinal arrangement of y and θ. (b) Comparison of two approaches for the stability analysis of this system ($V=0, L=20, 0.1\leqslant\gamma\leqslant 0.8$) subject to control (2). The first and second leading eigenvalues of the Jacobian matrices of the infinite-gain frozen-θ reduced model [Eq. (10a)] are denoted by solid and broken lines while the eigenvalues of the finite-gain closed-loop frozen-θ model ($\lambda^*=0, y^*=0$) with gains of $k=-1$ and -20 are denoted by circles and points, respectively.

We refer to single-variable systems as those with a fixed activity ($\theta=1$) while in a two-variables system the second variable (θ) is slow (ε is the ratio of time scales) and nondiffusing, and its kinetics is described by

$$\theta_t = \varepsilon Q(y,\theta). \tag{1b}$$

The interaction of these two variables led to complex spatiotemporal patterns that were investigated extensively by us, as well as by others, for the three situations described here: Sheintuch and Nekhamkina [20] studied the adiabatic reactor, Nekhamkina *et al.* [21] studied the cross-flow reactor. Numerous studies of the diffusion-reaction system, which represent many physical systems including the catalytic wire, were summarized in monographs [18,19]. Sheintuch [22] and Middya *et al.* [23] studied the catalytic wire under global control.

We are interested in controlling a stationary front [e.g., Fig. 1(a)], the steady solution of Eq. (1). Initially, we limit the study to the case of a wide separation of time scales ($\varepsilon \ll 1$), for which we can assume the $\theta_s(z)$ profile to be frozen over short times. Model (1) exhibits front solutions that may become unstable due to various interactions. Yet while analytical results exist for a single front in unbounded systems

with a polynomial source function [18,19], the behavior of a realistic bounded (finite-size) system with several fronts, and arbitrary bistable kinetics, cannot be predicted analytically in most cases.

A. Model reduction and linear analysis

The simplest control is based on a single sensor, located at z^* near the desired front position, and controlling one of the model parameters (λ). The control law is of the form

$$\lambda = \lambda^* + k[y(z^*) - y^*], \tag{2}$$

where y^* is the set point. To find the necessary gain, we reduce the model to a presentation that follows the change in front position, by approximating the front velocity (c): We envision a low state on the left and a high one on the right [Fig. 1(a)], and $c>0$ implies expansion of the latter. Thus, the front position is described by

$$\frac{dZ_f}{dt} = -c(V,\theta,\lambda) \sim V - c_{V=0}(\theta,\lambda). \tag{3}$$

The approximation above expresses the effect of convection that can be shown to push the front in the flow direction [16]. The front velocity is the resulting effect of convection and front velocity in the absence of convection. We assume also that changes in θ are slow so that $\theta = \theta_s(z)$ is the frozen steady-state solution. The typical steady y_s and θ_s profiles are presented in Fig. 1(a). Now the front is stationary for a certain $c^*(\theta_s^*, \lambda^*) = V$, that is, under conditions that the kinetic front counteract the convective force. We expand now

$$c_{V=0}(\theta_s, \lambda) = c^*(\theta_s^*, \lambda^*) + \left(\frac{\partial c}{\partial \theta}\right)_f [\theta_s(Z_f) - \theta_s^*] + \frac{\partial c}{\partial \lambda}(\lambda - \lambda^*) \tag{4}$$

to find the dependence of the front position on activity and on the control variable. Since θ is assumed to be frozen for the short perturbation times we consider, we can write

$$\theta_s(Z_f) - \theta_s^* = \left(\frac{\partial \theta}{\partial z}\right)_f (z - Z_s) = \left(\frac{\partial \theta}{\partial z}\right)_f (Z_f - Z_s), \tag{5}$$

where the subscript f denotes the front position. Moreover, gradients in y and θ are related by

$$\left(\frac{\partial \theta}{\partial z}\right)_f = -\frac{Q_y}{Q_\theta}\left(\frac{\partial y}{\partial z}\right)_f. \tag{6}$$

Similarly, the control effect can be expressed in a similar form where we typically place the sensor (z^*) at the desired steady front position (Z_s),

$$\lambda = k(y - y^*) = -\left(\frac{\partial y}{\partial z}\right)_f (Z_f - Z_s), \tag{7}$$

and the front velocity for $\lambda^* = 0$, $V = 0$, is described by

$$-\frac{dZ_f}{dt} = c(Z_f) = c_{V=0}(\theta_s^*) - \left[\left(\frac{\partial c}{\partial \theta}\right)_f \frac{Q_y}{Q_\theta} + k\frac{\partial c}{\partial \lambda}\right]\left(\frac{\partial y}{\partial z}\right)_f (Z_f - Z_s) \tag{8}$$

and the critical gain is readily approximated.

Example 1. For the simple cubic $P(y,\theta,\lambda) = -y^3 + y + \theta + \lambda$, $Q(y,\theta) = \varepsilon(-\gamma y - \theta)$, and $V = 0$, $\lambda^* = 0$, for which an analytical solution exists for a sufficiently long system, the problem is reduced, after incorporating the $Q(y,\theta)$ kinetics into Eq. (8) and noting that $\partial c/\partial\theta = \partial c/\partial\lambda$, to $k < -\gamma$ ($\partial c/\partial\theta = \partial c/\partial\lambda > 0$).

Testing the control in the limit of infinite (positive or negative) gain (k) amounts to pinning the solution so that

$$y(z^*) = y^*.$$

The ability of this controller to stabilize the system can be checked now by replacing the original problem with the following two problems that describe the system upstream and downstream of the front:

$$y_t - y_{zz} + V y_z = P(y, \theta_s(z), \lambda^*),$$

$$y_z|_{z=0} = V(y|_{z=0} - y_{\text{in}}), \quad y|_{z^*} = y^*; \tag{9a}$$

$$y_t - y_{zz} + V y_z = P(y, \theta_s(z), \lambda^*), \quad y|_{z^*} = y^*, \quad y_z|_{z=L} = 0. \tag{9b}$$

To find the eigenvalues, linearize the problem within each domain,

$$\overline{y}_t - \overline{y}_{zz} + V\overline{y}_z = P_y(y_z(z), \theta_s(z), \lambda^*)\overline{y},$$

and use spectral methods to expand $\overline{y} = y - y_s = \Sigma a_l \phi_i(i\pi z/L + z^0)$, where $y_s = y_s(z)$ is the steady solution, $\overline{y} = y(z,t) - y_s$ is the deviation, and the wave number i and z^0 are determined by the boundary conditions, to convert the problem into a set of linear ODE's.

Example 1a. For the simple kinetics (and $V = 0$) described in example 1, the solution exhibits inversion symmetry around midpoint and it is sufficient to study $y_t - y_{zz} = -y^3 + y + \theta_s(z)$ within the half-domain $0 < z < L/2$, subject to $y_z|_{z=0} = 0$, $y|_{z=L/2} = 0$. Approximation of the linearized system by the spectral methods leads to a set of ODE's,

$$a_t = Aa,$$

$$A_{ij} = -\frac{(2i-1)^2\pi^2}{L^2}\delta_{ij} + \langle(-3y_s^2 + 1)\phi_i, \phi_j\rangle,$$

$$i,j = 1,2,\ldots, \tag{10a}$$

where $\delta_{ij} = 1$ when $i = j$ and $\delta_{ij} = 0$ otherwise. The ϕ_i's eigenfunctions are calculated from the linearized problem $\overline{y}_t - \overline{y}_{zz} = (-3y_s^2 + 1)\overline{y}$, which leads to eigenvalues and eigenfunctions of the problem, $\phi_{zz}(z) = -\lambda\phi(z)$, $\phi_z(0) = \phi(L/2) = 0$,

$$\lambda_i=\frac{(2i-1)^2\pi^2}{L^2},$$

$$\phi_i(z)=\frac{2}{\sqrt{L}}\cos\left(\frac{(2i-1)\pi z}{L}\right),\quad i=1,2,\ldots \tag{10b}$$

(see the Appendix).

For evaluating A_{ij} we can approximate the steady-state solution of PDE (1) $[-y_{szz}=-y_s^3+y_s(1-\gamma)]$ with the analytical results of a long system: $y_s=\sqrt{1-\gamma}\tanh[(z-z_f)\sqrt{0.5(1-\gamma)}]$ obtained by rescaling of the single-variable problem, $-y_{szz}=-y_s^3+y_s$, $y_{sz}|_{0,L}=0$, which in turn has a well-known solution (for an infinitely long system) $y_s=\tanh(z/\sqrt{2})$ [19]. By integrating Eq. (10a) with $z_f=L/2$, we obtain

$$A_{ii}=1-\frac{6\beta^2}{L}\left\{\frac{L}{2}-\frac{\sqrt{2}}{\beta}\tanh\left(\frac{\beta L}{2\sqrt{2}}\right)+4\sqrt{2}\beta\left(\frac{1+e^{-0.5L\sqrt{2}\beta}}{2\beta^2+4\lambda_i}-2\frac{1+e^{-L\sqrt{2}\beta}}{8\beta^2+4\lambda_i}\right)\right\}, \tag{11a}$$

$$A_{ij}=-\frac{24\sqrt{2}\beta^3}{L}\left(\frac{1+e^{-0.5L\sqrt{2}\beta}}{2\beta^2+4q_1}-2\frac{1+e^{-L\sqrt{2}\beta}}{8\beta^2+4q_1}+\frac{1+e^{-0.5L\sqrt{2}\beta}}{2\beta^2+4q_2}-2\frac{1+e^{-L\sqrt{2}\beta}}{8\beta^2+4q_2}\right), \tag{11b}$$

where $\beta=\sqrt{1-\gamma}$, $q_1=(i+j-1)^2\pi^2/L^2$, and $q_2=(i-j)^2\pi^2/L^2$ (see the Appendix for derivation and the general formula for A_{li},A_{ij} when $z_f\neq L/2$).

The comparison of two approaches, both assuming a frozen-θ profile either with an infinite or with a finite gain, is presented in Fig. 1(b): The leading eigenvalues of matrix A (solid and broken lines, truncated order $N=14$) from Eq. (10a), where we assumed an infinite gain and a frozen-θ profile [Fig. 1(a)], are compared for various γ values with those of the Jacobian matrix of the lumped model of PDE's (1), again with a frozen-θ profile, controlled by $\lambda=k[y(z^*)-y^*]$ [Eq. (2) with $\lambda^*=0$, $y^*=0$] with a gain of $k=-1$ (circles) or $k=-20$ (points). Figure 1(b) shows the similarity of slow dynamics of these models when the gain is sufficiently high (practically $|k|>1$). This supports the adequacy of the reduced model (9) and its efficiency for analysis of the closed-loop system with pinning control.

Both models demonstrate the inefficiency of pinning control for $\gamma>\frac{2}{3}$. That results from the effect of γ on the phase plane: For $\gamma<\frac{2}{3}$, the system $P=Q=0$ exhibits bistability (two stable states) and the distributed system exhibits a front that separates them. For $\gamma>1$ and $\varepsilon\ll 1$, the system exhibits a unique unstable state surrounded by a limit cycle while for $\frac{2}{3}<\gamma<1$ the system exhibits bistability but the stability depends on ε (see the detailed analysis in [15]). To verify these conditions, note that the steady states of the ODE system $y_t=-y^3+y+\theta$, $\theta_t=\varepsilon(-\gamma y-\theta)$ are $y_s=\pm\sqrt{1-\gamma}$ and the corresponding eigenvalues are approximately $m_{1,2}=-(2-3\gamma+\varepsilon)/2\pm\sqrt{(2-3\gamma+\varepsilon)^2/4-(2-2\gamma)\varepsilon}$. Thus, for small ε the eigenvalues are $m_1=-2(1-\gamma)\varepsilon/(2-3\gamma+\varepsilon)$, $m_2=-(2-3\gamma+\varepsilon)-m_1$.

Example 2. For $V>0$ and $P(y,\theta_s,\lambda)=-(y^2-1)(y-a)+\theta_s+\lambda$, we can still find an analytical solution for the front velocity. To render the front stationary we set $a=-V/\sqrt{2}$. Such a source function admits an analytical steady-state solution in an infinitely long system, $y_s=\sqrt{1-\gamma}\tanh[(z-z_f)\sqrt{0.5(1-\gamma)}]$. To study the effect of infinite gain, we need to solve the two domains (9a) and (9b) (with the front in the center) for the upstream and downstream sections, which become for $\lambda^*=0$, $z^*=L/2$, and $y^*=0$,

$$y_t-y_{zz}+Vy_z=-(y^2-1)(y-a)+\theta_s(z),\quad y_z|_{z=0}=V(y|_{z=0}-y_{\rm in}),\quad y|_{z=L/2}=0; \tag{12a}$$

$$y_t-y_{zz}+Vy_z=-(y^2-1)(y-a)+\theta_s(z),\quad y|_{z=L/2}=0,\quad y_z|_{z=L}=0. \tag{12b}$$

The linearized problem of the upstream section (12a) $\overline{y_t}-\overline{y}_{zz}+V\overline{y}_z=(-3y_s^2+1+2ay_s)\overline{y}$ leads to the eigenvalues λ_i and eigenfunctions $\phi_i(z)$ [adjoint eigenfunctions $\phi_i^a(z)$] of the linear operator, $\phi_{zz}(z)-V\phi_z(z)=-\lambda\phi(z)$, subject to $\phi_z(0)=V\phi(0)$, $\phi(L/2)=0$,

$$\lambda_i=\sigma^2+\frac{V^2}{4},$$

$$\phi_i(z)=\Theta_i e^{0.5Vz}\left(\cos(\sigma_i z)+\frac{V}{2\sigma_i}\sin(\sigma_i z)\right),$$

$$\phi_i^a(z)=\phi_i(z)e^{-Vz} \tag{13}$$

with σ_i, $i=1,2,\ldots$ satisfying the equation $2\sigma_i=-Vtg(\sigma_i L/2)$, $\Theta_i=\langle[\cos(\sigma_i z)+(V/2\sigma_i)\sin(\sigma_i z)]^2\rangle^{-0.5}$ (see the Appendix for derivation).

The approximation of the linearized system by spectral methods leads to the following linear system in the domain $0<z<L/2$:

$$a_t=Aa,$$

$$A_{ij}=-\left(\sigma_l+\frac{V^2}{4}\right)\delta_{ij}+\langle(-3y_s^2+2ay_s+1)\phi_i\phi_j^a\rangle,\quad i,j=1,2,\ldots. \tag{14}$$

The downstream section is described by Eq. (12b) and yields the same eigenvalues and eigenfunctions as in Eq. (13) (see the Appendix).

Figure 2 compares the analysis of three approaches for various γ values (and $L=20$, $V=0.1$). The infinite-gain frozen-θ approach ($\varepsilon=0$) yields a leading eigenvalue [of matrix A, Eq. (14)] denoted by a solid line. The finite-gain, frozen-θ approach ($\lambda^*=0$, $y^*=0$, $k=-20$, truncation order $N=14$) yields the leading eigenvalue denoted by points, and the full model that accounts for varying θ ($\varepsilon=0.1$) yields the

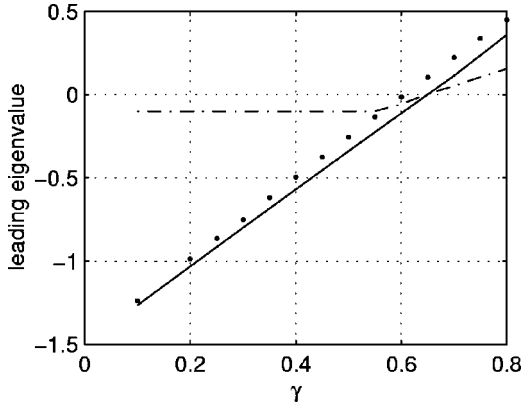

FIG. 2. Comparison of three approaches for the stability analysis of the 1D reaction-convection-diffusion system [Eq. (1), $V=0.1, L=20, 0.1\leqslant\gamma\leqslant 0.8$] subject to control (2): The leading eigenvalue of the Jacobian matrix of the infinite-gain frozen-θ reduced model [Eq. (14)] is denoted by the solid line while the leading eigenvalue of the finite-gain closed-loop frozen-θ model is denoted by points and that of the full ($\varepsilon=0.1$) model ($\lambda^*=0, y^*=0, k=-20$) is marked by a dashed-dotted line.

dashed-dotted line: As in Fig. 1(b), the frozen-θ models with finite or infinite k yield similar results. The full model predicts that the largest eigenvalue of the short system is negative for $\gamma<0.6$ as expected from the analysis of the homogeneous state [$\gamma<(2+\varepsilon)/3$, see example 1(b)]. All these models demonstrate that the pinning control is effective for $\gamma<\gamma^*(V)$ (Fig. 2).

III. PINNING PLANAR FRONTS

The structure of this section is as follows: Model reduction and various control strategies are analyzed in Sec. III A. Linear analysis and control design are outlined in Secs. III B and III C.

A. Model reduction and control strategies

Consider a reaction-diffusion problem in the (z,r) rectangular domain of length L and width R (e.g., see Fig. 3),

$$y_t - y_{zz} - y_{rr} = -y^3 + y + \theta + \lambda, \tag{15a}$$

$$\theta_t = \varepsilon(-\gamma y - \theta) \tag{15b}$$

subject to no-flux boundary conditions:

$$y_z(0,r)=0, \quad y_z(L,r)=0,$$

$$y_r(z,0)=0, \quad y_r(z,R)=0. \tag{15c}$$

We want to stabilize a 1D front in the middle (i.e., at $z=L/2$) of this 2D domain. One instability stems from the same reason as in the 1D problem, namely the anticlinal arrangement of the front and the slow variable [Fig. 1(a)]. However, while a single actuator can arrest the front in the 1D system, here the front, in a sufficiently wide system, may

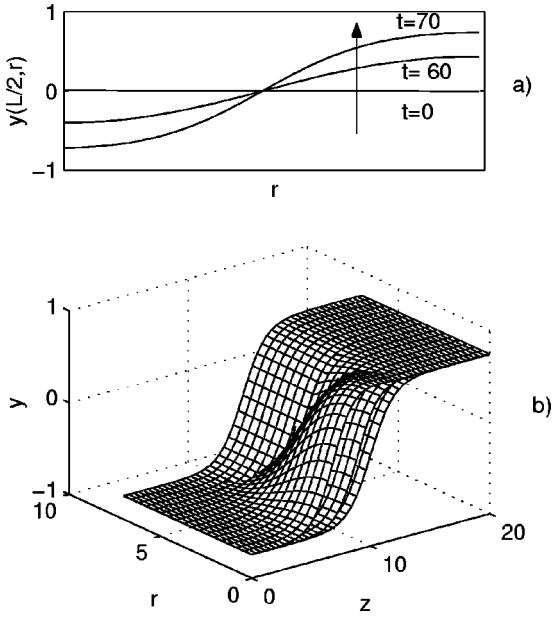

FIG. 3. Time evolution of the front line $y(L/2,r)$ (a) and of the planar front solution (b) of the closed-loop system (15) subject to the control law $\lambda=-20[y(z^*,r^*,t)-y_s(z^*,r^*)]$ with a single space-independent actuator located at the domain center ($z^*=L/2$, $r^*=R/2$; $L=20$, $R=7$, $\varepsilon=0.1$, and $\gamma=0.45$).

undergo symmetry breaking so that in part of it the upper state expands while in the other part the lower state propagates (see Fig. 3).

We begin the analysis with the case $\varepsilon\to 0$ so that $\theta=\theta_s(z)$ can be assumed to be the frozen steady state. The velocity of a planar front now depends on its curvature and with $K\ll 1$ it is [19]

$$c=c_\infty - DK, \quad K=f''/(1+f'^2)^{3/2}, \tag{16}$$

where c is the velocity in the direction perpendicular to the front, which is described by a certain curve $Z_f - Z_s = f(r)$, and c_∞ is the front velocity of a planar front in a large system; D is the diffusivity, which in our case is scaled into the length scale (i.e., $D=1$).

Now, consider perturbations of stationary fronts in the radial (r) direction and various control approaches.

(i) *Line actuator*. If we pin the whole front at the front line $Z_f(r)=L/2$ to $y=y^*$, then the problem is reduced to its one-dimensional analog as described above. That may not be a practical solution and we should look for pinning the front at few points along the front line.

(ii) *Point actuator*. If we place the sensor at the center of the domain $y^*=y(L/2,R/2)$ and use a simple uniform planar actuator, $\lambda=k(y-y^*)$, then for small deviations (the curvature for small deviations is $K=f''$) we have

$$-\frac{dZ_f}{dt} = -\frac{df(r)}{dt} = c(f(r))$$

$$= -\frac{Q_y}{Q_\theta}\left(\frac{\partial c}{\partial \theta}\right)_f \left(\frac{\partial y}{\partial z}\right)_f f(r) - \frac{\partial^2 f}{\partial r^2} - \frac{\partial c}{\partial \lambda}\left(\frac{\partial y}{\partial z}\right)_f k f\left(\frac{R}{2}\right). \tag{17a}$$

(iii) *Finding critical R*. With a sufficiently large gain, we can pin the front at its center but that may not be sufficient in a wide system. We should consider fronts that admit no-flux boundary conditions, i.e., $f\sim\cos(n\pi r/R)+\delta$, $n=1,2,\ldots,$ where δ is a certain constant value. The most unstable perturbation is that with $n=1$, and therefore

$$-\frac{dZ_f}{dt}=-\frac{df(r)}{dt}=c(f(r))=-\frac{Q_y}{Q_\theta}\left(\frac{\partial c}{\partial\theta}\right)_f\left(\frac{\partial y}{\partial z}\right)_f f(r)-\frac{\partial^2 f}{\partial r^2}. \tag{17b}$$

Setting $f\sim a_n(t)\cos(n\pi r/R)+\delta$, we can approximate the eigenvalues of this problem as

$$m_n=\gamma c_{\theta f}y_{zf}-(n\pi/R)^2,\quad c_{\theta f}=(\partial c/\partial\theta)_f \tag{18}$$

and we find that for R larger than a critical value this approach cannot assure the stability of this state. For example, the front velocity c_∞ of Eq. (15a) with the frozen profile $\theta=\theta_s(z)$ is $c_\infty=(y_+ +y_- -2y_i)$ [19], where y_+, y_-, y_i are roots of $-y^3+y=0$. Calculating c_∞ at the front position as $c_{\infty f}\cong 3(\theta_s+\lambda)/\sqrt{2}$ (see details in [14]) we obtain $c_{\theta f}\cong 3/\sqrt{2}$. The derivative y_{zf} may be evaluated by differentiation of the analytical steady-state solution, $y_s=\sqrt{1-\gamma}\tanh[(z-Z_f)\sqrt{(1-\gamma)/2}]$ as $y_{zf}=(1-\gamma)/\sqrt{2}$. Then the leading eigenvalue of the problem (17b) with $\gamma=0.45$ is $m_1=0.37-(\pi/R)^2$ from which we calculate the critical

$$R_{\rm cr}=5.16.$$

This $R_{\rm cr}$ is a good approximation for the value obtained below by other methods for the full PDE's (15) with $\varepsilon=0.1$.

(iv) *Two actuators*. Now, for $R>R_{\rm cr}$ we have to turn to a control based on two sensors and two actuators: From the nature of the unstable perturbations which admit no-flux boundary conditions, we should impose a control that in the model reduction appears in the form $\cos(n\pi r/R)+\delta$, where δ is a certain constant value; i.e., in the original system the simplest two-actuator control is of the form

$$\lambda=k_1y_1+k_2y_2\cos(\pi r/R), \tag{19}$$

where $y_i=y(r_i)$ is measured at the points $(L/2,r_i)$. Control λ in Eq. (19) is determined from the perturbations of y at two sensors located at $(L/2,r_1)$, $(L/2,r_2)$. This control responds to deviations in the front position because $y(L/2,r_i)\cong -f(r_i)$, where $f(r_i)=(Z_f-Z_s)|_{r_i}$, $i=1,2$. To study the effectiveness of this actuator, substitute control (19) into Eq. (17a) to find a term like $(\partial c/\partial\lambda)(\partial y/\partial z)(\lambda-\lambda^*)$ instead of $kf(R/2)$. We obtain that with a certain k_1, the eigenvalues of this problem are approximated by $m_n=\gamma c_{\theta f}y_{zf}-(n\pi/R)^2-k_2y_2$. They can be shifted to the negative domain by a sufficiently large gain k_2.

(v) *Many actuators*. Obviously, with increasing width of the system we will have to employ more sensors and more actuators. In that case we suggest using several sensors located along the front at preset positions $(z,r)=(L/2,r_d)$, $d=1,\ldots,\eta$ and apply a general feedback control law of the form

$$\lambda=\lambda^*+k\sum_{d=1}^{\eta}[y(L/2,r_d,t)-y_d^*]\psi_d(z,r), \tag{20}$$

where $y(L/2,r_d,t)-y_d^*$ are deviations of the sensors from the set points $y_d^*=y^*(L/2,r_d)$; $\psi_d(z,r)$ are some space-dependent functions that may imitate the eigenfunctions. For design of control (20) we apply below the general approach based on Liapunov's linearization method and the advanced linear system theory [24]. This approach uses a linearized lumping model of PDE's and is best suitable for a systematic computer-aided search of the regulator form. Moreover, the method may be applied to PDE's (1) without the analysis limiting to the time-scale separation and to the forms of perturbation. We will seek control (20) with the simplest space-independent or space-dependent actuator functions $\psi_d(z,r)$.

Below we consider in detail the theoretical basis for the design of linear feedback control (20).

B. Linear analysis

Linearizing system (15) for $\lambda=0$ around $y_s=y_s(z,r)$, $\theta_s=\theta_s(z,r)$, the steady-state solution, we find

$$\overline{y}_t-\overline{y}_{zz}-\overline{y}_{rr}=(-3y_s^2+1)\overline{y}+\overline{\theta}+\lambda, \tag{21a}$$

$$\overline{\theta}_t=-\varepsilon\gamma\overline{y}-\varepsilon\overline{\theta}. \tag{21b}$$

We use the Galerkin approach for lumping these equations with λ from Eq. (20) by expanding the deviations $\overline{y}(z,r,t)$, $\overline{\theta}(z,r,t)$, and $\overline{y}(z^*,r_d,t)=y(z^*,r_d,t)-y_s(z^*,r_d)$ as

$$\overline{y}(z,r,t)=\sum_e a_e(t)\phi_e(z,r),$$

$$\overline{y}(z^*,r_d,t)=\sum_e a_e(t)\phi_e(z^*,r_d),$$

$$\overline{\theta}(z,t)=\sum_e b_e(t)\phi_e(z,r), \tag{22}$$

where $z^*=L/2$. The orthonormal functions $\phi_e(z,r)$ are the eigenfunctions of the problem,

$$\phi_{zz}(z,r)+\phi_{rr}(z,r)=-\lambda\phi(z,r),$$

$$\phi_z(0,r)=\phi_z(L,r)=\phi_r(z,0)=\phi_r(z,R)=0 \tag{23}$$

with the eigenvalues

$$\lambda_{e(ij)}=\left[\frac{(i-1)^2}{L^2}+\frac{(j-1)^2}{R^2}\right]\pi^2 \tag{24a}$$

and the eigenfunctions

$$\phi_{e(ij)}(z,r)=\frac{\rho}{\sqrt{LR}}\cos\frac{(i-1)\pi z}{L}\cos\frac{(j-1)\pi r}{R},$$

$$e=e(ij)=1,2,\ldots, \tag{24b}$$

where $\rho=1$ when $i=j=1$, $\rho=2$ when $i, j>1$, and $\rho=\sqrt{2}$ when $i=1, j>1$ or $j=1, i>1$ [see the Appendix for a derivation of Eq. (24)].

Approximation by spectral methods of Eqs. (21a), (21b), and (20) with $\lambda^*=0$ and set points $y_d^*=y_s(z^*,r_d)$ leads to the infinite system of ODE's,

$$\dot{a}_e=-\lambda_e a_e+\sum_m J_{em}a_m+b_e + k\sum_{d=1}^{\eta}\int_0^L\int_0^R \psi_d(z,r)\sum_f a_f\phi_{f(kl)}(z^*,r_d) \times\phi_{e(kl)}(z,r)dz\,dr, \tag{25}$$

$$\dot{b}_e=-\varepsilon(\gamma a_e+b_e), \tag{26}$$

where

$$J_{em}=\int_0^L\int_0^R(-3y_s^2+1)\phi_{m(ij)}\phi_{e(kl)}dz\,dr, \quad e,m=1,2,\ldots. \tag{27}$$

Let us evaluate the last sum in Eq. (25). Denoting

$$h_{df}=\phi_f(z^*,r_d), \tag{28}$$

we can present a term of this sum as

$$\int_0^L\int_0^R\psi_d(z,r)\sum_f a_f\phi_{f(kl)}(z^*,r_d)\phi_{e(kl)}(z,r)dz\,dr = \int_0^L\int_0^R\psi_d(z,r)\phi_{e(kl)}(z,r)dz\,dr\sum_f a_f h_{df}$$

and rewrite Eq. (25) with the notation

$$\beta_{ed}=\int_0^L\int_0^R\psi_d(z,r)\phi_{e(kl)}(z,r)dz\,dr \tag{29}$$

as follows:

$$\dot{a}_e=-\lambda_e a_e+\sum_m J_{em}a_m+b_e+k\sum_{d=1}^{\eta}\beta_{ed}\sum_f a_f h_{df}, \quad e,f=1,2,\ldots. \tag{30}$$

Closed-loop ODE's (30) and (26) may be presented in the usual vector-matrix form

$$\begin{bmatrix}\dot{\mathbf{a}}\\ \dot{\mathbf{b}}\end{bmatrix}=\begin{bmatrix}-\Lambda+J & I\\ -\varepsilon\gamma I & -\varepsilon I\end{bmatrix}\begin{bmatrix}\mathbf{a}\\ \mathbf{b}\end{bmatrix}+k\begin{bmatrix}\beta\\ O\end{bmatrix}[H \quad O]\begin{bmatrix}\mathbf{a}\\ \mathbf{b}\end{bmatrix}$$

or as an open-loop system with η-dimensional input v and output w,

$$\begin{bmatrix}\dot{\mathbf{a}}\\ \dot{\mathbf{b}}\end{bmatrix}=\begin{bmatrix}-\Lambda+J & I\\ -\varepsilon\gamma I & -\varepsilon I\end{bmatrix}\begin{bmatrix}\mathbf{a}\\ \mathbf{b}\end{bmatrix}+\begin{bmatrix}\beta\\ O\end{bmatrix}v, \tag{31}$$

TABLE I. Evolution of the truncated order N versus R ($L=20$).

R	1,2	3	4,5	6	7	8	9	10
N	9	14	16	22	23	27	29	30

$$w=H\mathbf{a} \tag{32}$$

closed by a high gain output feedback control

$$v=kI_\eta w, \tag{33}$$

where $\mathbf{a}(t)=[a_e]$, $\mathbf{b}(t)=[b_e]$ are the infinite-dimensional vectors ($e=1,2,\ldots$); v and w are finite-dimensional η-vectors, the matrix $\beta=[\beta_{ed}]$ has η infinite-dimension columns ($e=1,2,\ldots;d=1,\ldots,\eta$) and the matrix $H=[h_{df}]$ has η infinite-dimension rows ($d=1,\ldots,\eta,f=1,2,\ldots$); I_η is an unity $\eta\times\eta$ matrix; $\Lambda=\mathrm{diag}(\lambda_1,\lambda_2,\ldots)$, $I=\mathrm{diag}(1,1,\ldots)$, $J=[J_{em}]$, $e,m=1,2,\ldots$ are infinite-dimensional matrices.

Let us study control system (31) with output (32). The problem can be stated as follows.

Problem. For the linearized infinite-dimensional ODE system (31) and (32) it is necessary to find a *high gain* (k) output feedback control (33), constructed by using input v and output w of minimal dimensions, such that the closed-loop system be asymptotically stable.

The design of the control law uses a finite-dimensional truncated version of ODEs (31) and (32). The evaluation of order N of the truncated ODE system consists of two main stages: First we evaluate M [$M=\max(i,j)$, Eqs. (24a) and (24b)] which defines the minimal threshold for basic eigenfunctions (22) in the z and r directions: For assigned value $M=2,3,\ldots$ we calculate $m=M^2$ eigenvalues $\lambda_{e(ij)}$ [Eq. (24a)] and eigenfunctions $\phi_{e(ij)}(z,r)$ [Eq. (24b)], $e=1,2,\ldots,m$ of the linear operator of PDE's (15), order the eigenfunctions in increasing values of the related $\lambda_{e(ij)}$, and then calculate the leading eigenvalues of the $2m\times 2m$ dynamics matrices of Eq. (31). M coincides with the minimal one that ensures the convergence of the leading eigenvalues with desirable accuracy. In the next stage we need to estimate the truncated order N as the minimal value of e [the number of ordered eigenfunctions $\phi_{e(ij)}(z,r)$ for assigned M] which guarantees the desired accuracy of the approximation. Analysis of the leading eigenvalues for different system width R showed that $M\sim 10$ is sufficient for N evaluations for the conditions defined below. The results of evolution N

TABLE II. Number of unstable eigenvalues in an open-loop system for different R ($L=20$).

R	Number of positive eigenvalues
$0<R\leqslant 5.6$	2
$5.6<R\leqslant 10$	4
$R>10$	$\geqslant 6$

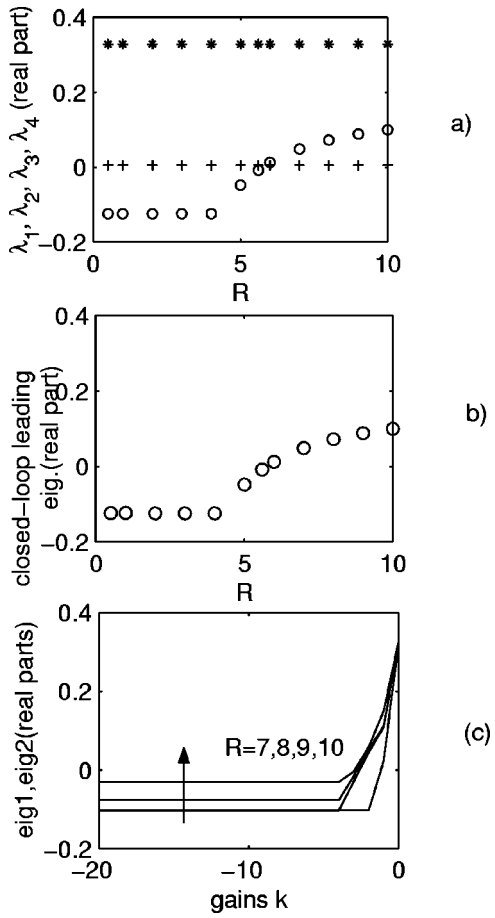

FIG. 4. The stability analysis of an open loop (a) and a closed loop system with one (b) or two (c) actuators: (a) The effect of the domain width (R) on the leading eigenvalues [λ_1 (asterisks), λ_2 (pluses), and real part of λ_3,λ_4 (circles)] of the open-loop system [truncated ODE system (31)]; (b) the effect of the domain width on the leading eigenvalues (real part, denoted by circles) of the closed-loop system [truncated ODE system (31) and (32)] with a high gain ($k=-20$) control (34) using a uniform actuator with a center-positioned sensor (other parameters as in Fig. 3, $M=10$); (c) effect of two actuators control [Eq. (35), $z^*=L/2, r_1=R/2, r_2=0, 7\leqslant R \leqslant 10$] on leading eigenvalues of the closed-loop truncated ODE system (31) and (32). Other parameters are as in Fig. 3.

versus R for assigned $M=10$ (Table I, $L=20$, $\varepsilon=0.1$, $\gamma=0.45$) show that N grows about linearly with R.

The stability analysis of the open-loop system for $M=10$ shows two real unstable eigenvalues of Eq. (31) (~ 0.328, ~ 0), which are identical to those of a narrow system and two complex eigenvalues with a real part that becomes positive for $R\geqslant 5.6$ [Fig. 4(a), parameters as in Table I]. Recall that this was approximated by the critical value predicted in Eq. (18). The number of unstable eigenvalues increases for $R>10$ (see Table II).

C. Control design based on the linearized lumped model

Control design implies the determination of the minimal number of actuators to be employed, their spatial form, and the location of the corresponding sensors that will assure the linear stability of the planar front. We start with a single simple (space-independent) actuator with a centrally positioned sensor. Assuming intuitively, as suggested by the model-reduction approach, that it is indeed the simplest sensor. When that fails in wide domains we demonstrate the methodological design of a two-actuator control. The proposed approach of control design uses the concepts of finite [24–26] and infinite zeros [27] of a linear multidimensional system (see [28,29] for details).

Simple single actuator control. We start by analyzing the effectiveness of the simplest control law: a single space-independent actuator [i.e., Eq. (20a) with $\eta=1$, $\psi_1(z,r)=1$]

$$\lambda = k[y(z^*, r_1, t) = y_s^*], \tag{34}$$

where $y_s^*=y_s(z^*,r_1)$.[1] The spectral representation of the closed-loop PDE's (15a), (15b), and (34) is a single-input single-output ODE's (31) and (32) with a column vector $\beta=[\beta_{11},0,0,\ldots]^T$ ($\beta_{11}=\sqrt{LR}$) and a row vector $H=h=[h_{11},h_{12},\ldots]$. We begin the analysis for an actuator that is situated at the domain center ($z^*=L/2, r_1=R/2$). The evolution of the leading eigenvalues with changing R in an open-loop and closed-loop ($k=-20$) system shows [Figs. 4(a) and 4(b)] that the high feedback influences only the two most positive leading eigenvalues ($\lambda_1\sim 0.328, \lambda_2\sim 0$) of the open-loop system while the next-leading (and complex) eigenvalues λ_3,λ_4 possess negative real parts for $0<R<5.6$ and positive real parts for $R\geqslant 5.6$. The critical width for the effectiveness of a simple actuator $R_{cr}\sim 5.5$ is in fair agreement with the model reduction prediction (see Sec. III A). The transition with increasing R is through a Hopf bifurcation, and simulations of the original system (15) with control (34) verify this by emergence of damped and undamped oscillations for R below and above this value [Figs. 5(a) and 5(b); $R=5.2,5.6$]. Figure 5 presents cross sections of the solution at $L/2$ (first column), temporal behavior of the center ($L/2,R/2$) position (second column), and the gray-scale plots of the state at $R/2$ (third column) and $L/2$ (fourth column).

Two-actuator control. It follows from Eq. (20) that while the form of the output matrix H is defined by the sensors number η and their positions [Eq. (28)], the form of the actuator functions $\psi_d(z,r)$ influences the structure of the matrix β [Eq. (29)]. Therefore, the general strategy of the method is based on assigning $\eta=1,2,\ldots$ preset actuator positions $(z,r)=(L/2,r_d)$, $d=1,\ldots,\eta$, by successively adding new corresponding rows in the $\eta\times N$ output matrix H and searching for the form of additional rows of the $N\times\eta$ matrix β such that the new β ensures stability of the closed-loop ODE's (31),(32) with a high gain control (33). The stability analysis may be fulfilled by directly calculating the leading eigenvalues of the above-mentioned closed-loop system versus gain coefficient k. But we use the advanced linear system theory to replace this procedure by the analysis of

[1]We propose that the set point y^* coincides with the desired steady-state value y_s^* of this problem.

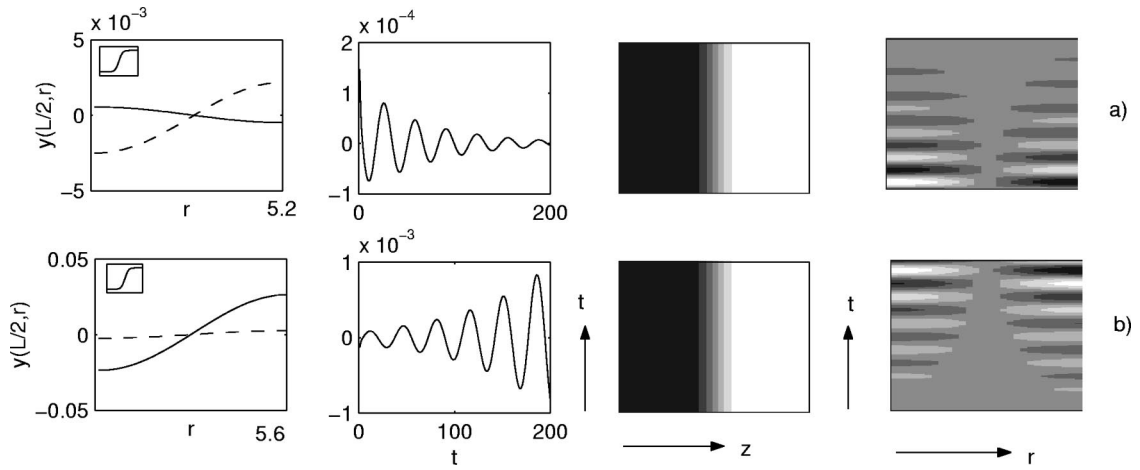

FIG. 5. (a),(b) Testing the effectiveness of control (34) with one space-independent actuator for system (15) of different widths: $R=5.2$ (a), $R=5.6$ (b). The figures present initial (dashed line) and final (solid line) y profiles in the r direction (column 1, insets are initial and final profiles in the z direction), the deviation of y from y_s in the center point $(L/2,R/2)$ (column 2), and gray-scale plots in the planes (t, z) at $r=R/2$ and in (t, r) at $z=L/2$ (columns 3 and 4). Initial perturbation in the r direction is $-0.01\cos(\pi r/R)$; the sensor is positioned at the center $(L=20,\varepsilon=0.1,\gamma=0.45,k=-20)$.

finite zeros and infinite zeros of open-loop system (31) and (32) applying the known property of a closed-loop linear system with a high gain feedback (see [24,27]): as the feedback gain increases towards infinity, part of the closed-loop eigenvalues remains finite and approaches the position which is referred to as the finite system zeros while the remainder are located at the points at infinity and are known as infinite zeros. Therefore, we propose to seek the suitable matrix β by the repeating calculations of the finite system zeros of open-loop ODE's (31) and (32) with different input matrices and finding one that ensures that the leading finite system zeros are negative. Then we need to rearrange the sensor position in the r direction so that the infinite zeros tend to infinity along asymptotes with a negative real axis angle. This is guaranteed if the eigenvalues of the $\eta\times\eta$ matrix $H\beta$ have real positive parts [27].

For simplification of the search of the matrix β structure, we may assign the eigenfunctions (24b) as actuator functions, i.e., $\psi_d(z,r)\sim\phi_e(z,r)$, $e=1,2,\ldots$; from the relation between the form of the actuator $\psi_d(z,r)$ functions and the structure of the matrix β [see Eq. (29)], it follows that every dth column of the matrix β will contain only nonzero element β_{ed}.

Apply control of the form

$$\lambda=k\sum_{d=1}^{2}[y(z^*,r_d,t)-y_s^*]\psi_d(z,r) \tag{35}$$

with one space-independent actuator $[\psi_1(z,r)=1]$ and another space-dependent one, $\psi_2(z,r)\sim\phi_e(z,r)$, that is, an eigenfunction from series (22) ordered in an increasing order of the appropriate eigenvalues.[2] Let us introduce two sensors at positions $(z^*=L/2,r_1)$, $(z^*=L/2,r_2)$ and calculate the $2\times N$ matrix H by formula (28). Then evaluating the system zeros of series systems (31) and (32) with output matrix H and different $N\times 2$ matrices

$$\beta=\begin{bmatrix}1/\sqrt{LR} & 0 & 0 & \cdots\\ \beta_{21} & \beta_{22} & \beta_{23} & \cdots\end{bmatrix}^T, \tag{36}$$

we may find β with the minimal number of nonzero elements β_{2i} which ensures the stability of the appropriate closed-loop system with a high gain. This matrix β contains nonzero elements $\beta_{11}\neq 0$, $\beta_{2i}\neq 0$ and the corresponding control (35) has one space-independent and one space-dependent actuator. For example, for PDE's (15) ($L=20$, $\gamma=0.45$, $\varepsilon=0.1$, $R=7$, $r_1=R/2$, $r_2=R$) the matrix β with $\beta_{24}\neq 0$ conforms to the ODE's having leading zeros with negative real parts (-0.1024). This β_{24} corresponds to the fourth eigenfunction $\phi_4\sim\cos(\pi r/R)$ in the ordered series of eigenfunctions.

Consequently control (35) becomes

$$\lambda=k\{[y(z^*,r_1,t)-y_s(z^*,r_1)]+[y(z^*,r_2,t)-y_s(z^*,r_2)]\cos(\pi r/R)\},\quad z^*=\frac{L}{2}. \tag{37}$$

Then we need to rearrange the sensor position in the r direction so that the eigenvalues of the 2×2 matrix $H\beta$ are positive. As was noted before, this guarantees that the infinite zeros tend to infinity along asymptotes with a negative real axis angle. For our example, we need to use r_i locations that satisfy the inequality $r_1>r_2$. The relevant matrix $H\beta$ with $r_1=R$ and $r_2=R/2$ has eigenvalues $0.0811\pm 0.8761i$. When $r_1<r_2$, the closed-loop high gain ODE's (31)–(33) are unstable: the matrix $H\beta$ has eigenvalues of $0.1161,-0.1226$.

The successful application of control (37) with $r_1=R$ and $r_2=R/2$ is demonstrated in Figs. 6(a) and 6(b). Further computation shows that it is able to stabilize the system with R

[2]The first six ordered eigenfunctions for PDE's (15) with $L=20$, $R=7$, $N=23$ are $\phi_1\sim 1,\phi_2\sim\cos(\pi z/L)$, $\phi_3\sim\cos(2\pi z/L)$, $\phi_4\sim\cos(\pi r/R)$, $\phi_5\sim\cos(3\pi z/L)$, $\phi_6\sim\cos(\pi z/L)\cos(\pi r/R)$.

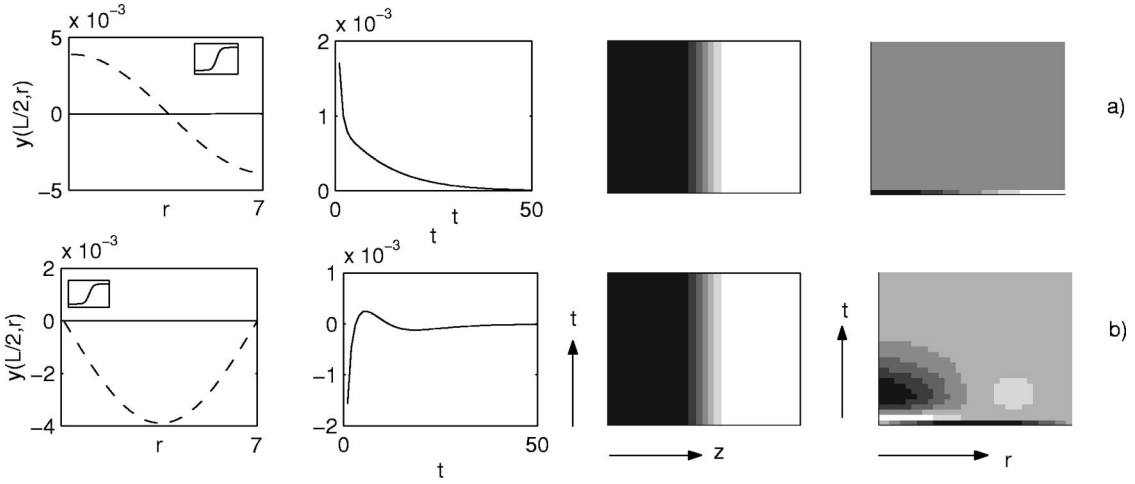

FIG. 6. (a),(b) Testing the effectiveness of control (37) with one state-independent and one state-dependent actuator for system (15) of width $R=7>R_{cr}$. The figure presents initial (dashed line) and final (solid line) y profiles in the r direction (column 1, insets are initial and final profiles in the z direction), deviation of y from y_s at point $(L/2,r_1)$ (column 2), gray-scale plot of y in the planes (t, z) at $r=R/2$ (column 3), and (t, r) at $z=L/2$ (column 4). Initial perturbation in the r direction is $0.01\cos(\pi r/R)$ in (a) and $-0.01\sin(\pi r/R)$ in (b); sensor positions are at $z^*=L/2$, $r_1=R$, and $r_2=R/2$. Other parameters as in Fig. 5.

$\leqslant 10$ [Fig. 4(c)]. Note that the structure of actuator (37) coincides with control law (19), which was derived from the reduced model.

We can use a similar approach for three or more actuators.

IV. CONCLUSION

The stabilization of planar stationary fronts in a two-dimensional rectangular domain, in which a diffusion-reaction systems occurs, is studied using a two-variable model incorporating a fast and diffusing activator with approximate (polynomial) kinetics, for which some analytical results are available, and a slow and localized inhibitor. We consider the simplest control strategy based on sensors placed at the front line position and measured deviations from a local state, and actuators that are spatially uniform or space-dependent. Large gains imply pinning the solution to one or few points.

We apply two approaches for control design: an approximate model reduction to a form that follows the front position while approximating the front velocity and assuming wide separation of activator-inhibitor time scales, and linear stability analysis. The same approaches were previously applied by us for analysis of one-dimensional systems. The approximate model reduction allows us to qualitatively analyze various control strategies and to predict the critical width below which the control mode of the one-dimensional system is sufficient. These results are corroborated by linear analysis of a truncated model with spectral methods representation, using concepts of finite and infinite zeros of linear multidimensional systems. We present a systematic control design that determines the number of required sensors and actuators, their position, and their form.

In a future presentation we will show how this know-how can be implemented to problems with convection. To that end we study the stabilization of planar fronts in a cylindrical annular reactor in which an oscillatory reaction occurs. Under the conditions studied the system exhibits a rotating pattern, but the incorporation of a simple pinning control, based on a sensor that measures the temperature at the front and an actuator that affects the feed concentration or the fluid velocity, is able to largely stabilize the front.

ACKNOWLEDGMENTS

This work was supported by the U.S.–Israel Binational Science Foundation. M.S. acknowledges the Minerva Center of Nonlinear Dynamics for support. Y.S. and O.N. are partially supported by the Center for Absorption in Science, Ministry of Immigrant Absorption, State of Israel.

APPENDIX

1. Derivation of Eqs. (10b) and (13)

The general solution of the problem

$$\phi_{zz}(z)=-\lambda\phi(z) \tag{A1}$$

with the nonflux b.c. is $\phi_i(z)=B_i\cos(\sqrt{\lambda_i}z)$ with $\lambda_i=(2i-1)^2\pi^2/L^2$. The coefficients B_i are chosen so that eigenfunctions be orthonormal; thus $B_i=2/\sqrt{L}$.

The eigenvalue problem

$$\phi_{zz}-V\phi_z=-\lambda\phi, \quad \phi_z(z)|_{z=0}=V\phi(0), \quad \phi(z)|_{z=L/2}=0 \tag{A2}$$

is a non-self-adjoint problem with adjoint eigenfunctions $\phi_i^a(z)=e^{-V}z\phi_i(z)$. We use the substitution

$$\phi_i(z)=e^{0.5V}zw_i(z) \tag{A3}$$

and obtain the self-adjoint eigenvalue problem

$$w_{izz}=\left(\lambda_i-\frac{V^2}{4}\right)w_i=0,$$

$$w_{iz}(z)|_{z=0} = Vw_i(0)/2,$$

$$w_i(z)|_{z=L/2} = 0. \tag{A4}$$

The general solution of problem (A4) is

$$w_i(z) = A_i \sin(\sigma_i z) + B_i \cos(\sigma_i z),$$

where $\sigma^2 = \lambda_i - V^2/4$. Application of the boundary conditions yields $A_i = -B_i ctg(\sigma_i L/2)$, where σ_i obeys the equation $2\sigma_i = -Vtg(\sigma_i L/2)$. As a result, we obtain the general solution of Eq. (A4) as $w_i(z) = B_i[\cos(\sigma_i z) + (V/2\sigma_i)\sin(\sigma_i z)]$. Substituting $w_i(z)$ in Eq. (A3) and choosing B_i to make the eigenfunctions orthonormal to adjoint eigenfunctions, we obtain Eq. (13).

2. Derivation of Eqs. (11a) and (11b)

From the orthonormal property of ϕ_i, we can express A_{ii} with $\beta = \sqrt{1-\gamma}$ as follows:

$$A_{ii} = \int_0^{L/2} (-3y_s^2 + 1)\phi_i^2 dz = \int_0^{L/2} -3y_s^2 \phi_i^2 dz + 1 = \int_0^{L/2} -3\beta^2 \tanh^2\left(\frac{\beta}{\sqrt{2}}(z - z_f)\right)\phi_i^2 dz + 1.$$

Since $\phi_i^2(z) = 4[\cos^2(qz)]/L = 2[1 + \cos(2qz)]/L$, $q = (2i-1)\pi/L$, we can rewrite the above expression as

$$A_{ii} = 1 - \frac{6\beta^2}{L}\left[\int_0^{L/2} \tanh^2\left(\frac{\beta}{\sqrt{2}}(z - z_f)\right) dz + \int_0^{L/2} \tanh^2\left(\frac{\beta}{\sqrt{2}}(z - z_f)\right) \cos\frac{2(2i-1)\pi z}{L} dz\right]. \tag{A5}$$

The first integral in Eq. (A5) is calculated exactly. For evaluating the second integral, we use the approximate expression for tanh: $\tanh y = \mathrm{sgn}(y)\{1 - 2\exp[-2abs(y)]\}$ [30], which for $y = z - z_f < 0$ takes the simple form

$$\tanh(z - z_f) = -1 + 2\exp[2(z - z_f)]. \tag{A6}$$

Substituting Eq. (A6), we can rewrite the last integral in Eq. (A5) in the form

$$\int_0^{L/2}\left[-4\exp\left(\frac{2\beta}{\sqrt{2}}(z - z_f)\right) + 4\exp\left(\frac{4\beta}{\sqrt{2}}(z - z_f)\right) + 1\right]\cos\frac{2(2i-1)\pi z}{L} dz \tag{A7}$$

and calculate A_{ii},

$$A_{ii} = 1 - \frac{6\beta^2}{L}\left\{\frac{L}{2} - \frac{\sqrt{2}}{\beta}\left(\tanh\frac{\beta(L/2 - z_f)}{\sqrt{2}} + \tanh\frac{\beta z_f}{\sqrt{2}}\right) + 4\sqrt{2}\beta\left(\frac{e^{\sqrt{2}\beta(-z_f + L/2)} + e^{-\sqrt{2}\beta z_f}}{2\beta^2 + 4\lambda_i} - 2\frac{e^{2\sqrt{2}\beta(-z_f + L/2)} + e^{-2\sqrt{2}\beta z_f}}{8\beta^2 + 4\lambda_i}\right)\right\}. \tag{A8}$$

From the orthonormal property of ϕ_i, ϕ_j $(i \neq j)$, we have

$$A_{ij} = \int_0^{L/2} (-3y_s^2 + 1)\phi_i\phi_j dz = \int_0^{L/2} -3y_s^2 \phi_i\phi_j dz = \int_0^{L/2} -3\beta^2 \tanh^2\left(\frac{\beta}{\sqrt{2}}(z - z_f)\right)\phi_i\phi_j dz.$$

Since

$$\phi_i(z)\phi_j(z) = \frac{2}{L}\left(\cos\frac{2(i+j-1)\pi z}{L} + \cos\frac{2(i-j)\pi z}{L}\right)$$

we can then rewrite A_{ij} as

$$A_{ij} = -\frac{6\beta^2}{L}\left[\int_0^{L/2} \tanh^2\left(\frac{\beta}{\sqrt{2}}(z - z_f)\right)\cos\frac{2\pi z}{L}(i+j-1) dz + \int_0^{L/2} \tanh^2\left(\frac{\beta}{\sqrt{2}}(z - z_f)\right)\cos\frac{2\pi z(i-j)}{L} dz\right].$$

For evaluating the integrals in the above expression we also use Eq. (A6). With the notation $q_1 = (i+j-1)^2\pi^2/L^2$, $q_2 = (i-j)^2\pi^2/L^2$, we obtain

$$A_{ij}=-\frac{24\sqrt{2}\beta^3}{L}\left(\frac{e^{\sqrt{2}\beta(-z_f+L/2)}+e^{-\sqrt{2}\beta z_f}}{2\beta^2+4q_1}-2\frac{e^{2\sqrt{2}\beta(-z_f+L/2)}+e^{-2\sqrt{2}\beta z_f}}{8\beta^2+4q_1}+\frac{e^{\sqrt{2}\beta(-z_f+L/2)}+e^{-\sqrt{2}\beta z_f}}{2\beta^2+4q_2}-2\frac{e^{2\sqrt{2}\beta(-z_f+L/2)}+e^{-2\sqrt{2}\beta z_f}}{8\beta^2+4q_2}\right). \tag{A9}$$

Formulas (11a) and (11b) follow from Eqs. (A8) and (A9) with $z_f=L/2$.

3. Derivation of Eq. (24)

Consider the general solution of the problem

$$\phi_{zz}(z,r)+\phi_{rr}(z,r)=-\lambda\phi(z,r) \tag{A10}$$

with the no-flux b.c.,

$$\phi_z(0,r)=\phi_z(L,r)=0, \quad \phi_r(z,0)=\phi_r(z,R)=0. \tag{A11}$$

We use a separation of variables, $\phi(z,r)=\Psi(z)\Omega(r)$, to obtain two one-dimensional Sturm-Liuvill problems,

$$\Psi_{zz}(z)=-\mu\Psi(z), \quad \Psi_z|_{z=0}=0, \quad \Psi_z|_{z=L}=0; \tag{A12}$$

$$\Omega_{rr}(r)=-\gamma\Omega(r), \quad \gamma=\lambda-\mu, \quad \Omega_r|_{r=0}=0, \ \Omega_r|_{r=R}=0. \tag{A13}$$

Problems (A12) and (A13) are similar to problems from [15] and have solutions for

$$\mu_i=\frac{(i-1)^2\pi^2}{L^2}, \quad \Psi_i(z)=\frac{B_i}{\sqrt{L}}\cos\frac{(i-1)\pi z}{L}, \quad B_1=1, \quad B_i=\sqrt{2}, \quad i>1, \tag{A14a}$$

$$\gamma_j=\frac{(j-1)^2\pi^2}{(R)^2}, \quad \Omega_j(r)=\frac{B_j}{\sqrt{R}}\cos\frac{(j-1)\pi r}{R}, \quad B_1=1, \quad B_j=\sqrt{2}, \quad j>1, \tag{A14b}$$

where $i,j=1,2,\ldots$. Using the equality $\gamma_j=\lambda-\mu_i$ and substituting the eigenfunctions from Eq. (A14) to $\phi(z,r)=\Psi(z)\Omega(r)$, we obtain Eq. (24).

[1] D. A. Frank-Kamenetski, *Diffusion and Heat Exchange in Chemical Kinetics* (Princeton University Press, Princeton, NJ, 1955).
[2] A. Burghardt, M. Berezowski, and E. W. Jacobsen, Chem. Eng. Process. **38**, 19 (1999).
[3] J. Puszynski, J. Degreve, and V. Hlavacek, Ind. Eng. Chem. Res. **26**, 1424 (1987).
[4] W. Marquardt, Int. Chem. Eng. **30**, 585 (1990).
[5] A. G. Merzhanov and E. N. Rumanov, Rev. Mod. Phys. **71**, 1173 (1999).
[6] M. Sheintuch and S. V. Shvartsman, AIChE J. **42**, 1041 (1996).
[7] M. Sheintuch and O. Nekhamkina, AIChE J. **45**, 398 (1999).
[8] M. Bar, I. G. Kevrekidis, H. H. Rotermund, and G. Ertl, Phys. Rev. E **52**, 5739 (1995).
[9] A. Kienle, Chem. Eng. Sci. **55**, 1817 (2000).
[10] A. Armaou and P. D. Christofides, AIChE J. **47**, 79 (2001).
[11] W.-J. Rappel, F. Fenton, and A. Karma, Phys. Rev. Lett. **83**, 456 (1999).
[12] V. Panfilov and M. Sheintuch, Chaos **9**, 78 (1999).
[13] V. Panfilov and M. Sheintuch, AIChE J. **47**, 187 (2001).
[14] M. Sheintuch and O. Nekhamkina, Phys. Rev. E **63**, 056120 (2001).
[15] Ye. Smagina, O. Nekhamkina, and M. Sheintuch, Ind. Eng. Chem. Res. **41**, 2023 (2002).
[16] M. Sheintuch, Ye. Smagina, and O. Nekhamkina, Ind. Eng. Chem. Res. **41**, 2136 (2002).
[17] S. Y. Shvartsman and I. G. Kevrekidis, AIChE J. **44**, 1579 (1998).
[18] P. C. Fife, *Mathematical Theory of Reacting and Diffusing Systems* (Springer-Verlag, Berlin, 1979).
[19] A. S. Mikhailov, *Foundations of Synergetics. I: Distributed Active Systems* (Springer-Verlag, Berlin, 1994).
[20] M. Sheintuch and O. Nekhamkina, Chem. Eng. Sci. **54**, 4535 (1999).
[21] O. A. Nekhamkina, B. Y. Rubinstein, and M. Sheintuch, AIChE J. **46**, 1632 (2000).

[22] M. Sheintuch, Chem. Eng. Sci. **44**, 1081 (1989).
[23] U. Middya, D. Luss, and M. Sheintuch, J. Chem. Phys. **100**, 3568 (1994).
[24] T. Kailath, *Linear Systems* (Prentice-Hall, Englewood Cliffs, NJ, 1980).
[25] Ye. Smagina, Autom. Remote Control (Engl. Transl.) **46**, 1493 (1985).
[26] C. B. Schrader and M. K. Sain, Int. J. Control **50**, 1407 (1989).
[27] B. Kouvaritakis and J. M. Edmunds, Int. J. Control **29**, 303 (1979).
[28] H. H. Rosenbrock, *State-Space and Multivariable Theory* (Wiley Interscience, New York, 1970).
[29] Ye. Smagina, *Problems of Linear Multivariable System Analysis Using the Concept of System Zeros* (Tomsk State University, Tomsk, 1990).
[30] J. Spanier and K. B. Oldham, *An Atlas of Functions* (Springer-Verlag, Berlin, 1987).